ADVANCED THERAPEUTICS
www.advtherap.com

Nanoprobes for PET/MR Imaging

*Huanhuan Liu, Runze Wang, Haiyan Gao, Lijuan Chen, Xiaochen Li, Xuan Yu, Yaping Wu, Yan Bai, Wei Wei, and Meiyun Wang**

The development of clinical imaging techniques significantly improves diagnostic accuracy and provides guidance for personalized treatment of individuals. However, every single imaging modality has its distinct drawbacks that cannot fully fulfil the diagnosis requirement. Thus, rational combination of different imaging modalities can achieve more comprehensive information of disease and in this way provide better personalized treatment strategy. The hybrid PET/MRI has drawn increasing attention since its first clinical application. Imaging probes play an essential role in achieving qualified figures with accurate information of diseases. The application of nanotechnology promotes the development of versatile molecular probes for PET/MRI technique. Though there is an emerging clinical requirement, only a small number of multimodal PET/MRI probes have been investigated in preclinical research. Thus, this review tries to thoroughly summarize the nano-sized PET/MRI probes on their design, preparation and biological application. By discussing the strength and limitations of these current available PET/MRI multimodal probes, this work aims to figure out the further research direction and promote the possible clinic translation of the novel PET/MRI probes.

1. Introduction

Imaging techniques play essential roles in diagnosis and even treatment of disease. Nowadays, the mainstream imaging technologies used in hospitals include magnetic resonance imaging (MRI), X-ray computed tomography (CT), positron emission tomography (PET), single-photon emission computed tomography (SPECT), ultrasound (US) imaging and so on. However, each single imaging modality has its instinct limitation, which would lead to either poor detection sensitivity or low diagnosis accuracy.[1] To overcome these disadvantages of single technique, combination of imaging modalities can integrate the advantages of each single imaging technique and thus provide new opportunities for better diagnosis strategies.[2,3] The combination of PET and MRI, namely PET/MRI, has emerged as a powerful tool in disease diagnosis since the first whole-bodyhuman Positron Emission Tomograph/Magnetic Resonance Imaging (PET/MRI) system come to the clinic in 2010.[4]

The MRI is a non-invasive imaging technique with high image resolution. MRI makes use of the motion of nuclear magnetic spins in nuclides for data acquisition. ^{1}H in water molecule is one of the most MRI-active nuclides. Regarding the fact that Water makes up more than 70% of human mass, MRI can give plenty of information on the human body.[5] Comparing with other imaging technique, MRI has the superior ability for the visualization of soft tissues, such as brain and central nervous system.[6,7] To acquire images with high quality, MRI contrast reagents are commonly used for enhancing the contrast resolution between the lesion site and healthy tissue. Gadolinium-based contrast agents (GBCA), such as Gadobutrol and Gadoteric acid are commonly applied to increase the information content of MRI images.[8] After being intravenously injected, the GBCA accumulate at the interesting spot as a result of in vivo circulation and therefore provides diagnostic information. However, the disadvantages such as nephrogenic systemic fibrosis (NSF) and gadolinium retention raise the concern of severe side effects during the application of GBCA.[9] Currently, superparamagnetic iron oxide nanoparticles, such as ferumoxytol, has been considered as one of the alternatives of GBCA, and showed a very promising clinical perspective. Besides, some novel materials, such as manganese-based materials and soft nanoparticle have also been widely studied as the MRI contrast reagent.

Positron Emission Tomography (PET) is another non-invasive medical imaging technique with high sensitivity and the capacity of quantitative analysis. The image acquisition of PET is based on the detection of high-energy gamma-ray photons generated by the annihilation of positrons which produced by β^{+}-emitting radioisotope.[10] The positron emitting isotopes, for instance, ^{18}F, ^{14}C, ^{68}Ga, and ^{64}Cu are commonly used for PET imaging.[11]

H. Liu, H. Gao, L. Chen, X. Li, X. Yu, Y. Wu, Y. Bai, W. Wei, M. Wang
Department of Medical Imaging
Henan Provincial People's Hospital & the People's Hospital of Zhengzhou University
Zhengzhou 450003, P. R. China
E-mail: mywang@zzu.edu.cn
R. Wang
Department of Radiation Science and Technology
Delft University of Technology
Mekelweg 15, Delft 2629 JB, The Netherlands
M. Wang
Laboratory of Brain Science and Brain-Like Intelligence Technology
Institute for Integrated Medical Science and Engineering
Henan Academy of Sciences
Zhengzhou 450003, P. R. China

The ORCID identification number(s) for the author(s) of this article can be found under https://doi.org/10.1002/adtp.202300232

DOI: 10.1002/adtp.202300232

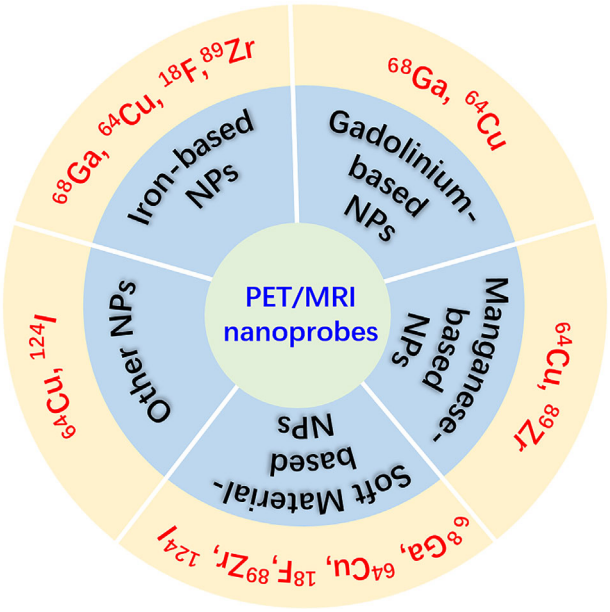

Scheme 1. PET/MRI probes that combined MRI reagents with PET radioisotopes.

Molecular probe ^{18}F-Fluorodeoxyglucose (FDG) is among the first-line of clinical PET probes. As a radioactive derivative of glucose, it is can give information on abnormalities based on the tissue metabolic activity and in this way tests the functionality of the tissue. Generally, PET is combined with CT for the acquisition of both functional information and anatomical information of diseases.[12]

Compared to PET/CT, PET/MRI techniques would produce low ionizing radiation doses for patients and get superior soft tissue information.[8] PET/MR technique show its advantages on the diagnosis of certain diseases, such as cardiovascular diseases and neurodegenerative disease. For better application of PET/MRI, the hybrid molecular probes have been widely studied, the applicable probes should meet some important criteria, such as low toxicity, good metabolic stability, favorable pharmacokinetic properties, which makes it quite challenging for the probe design.[5] The nanomaterials could be emerged as an excellent platform for the PET/MRI dual-modality imaging. By tuning the composition, size, surface modification and other factors, nano-sized materials can be given versatile functions. The fabrication of nano PET/MRI probes can be briefly summarized into two strategies: radiolabeling the nanosized MRI contrast reagents with PET radionuclides or integrating the MRI contrast reagents and radionuclides within the nanocarriers. In this review, we try to introduce the PET/MRI probes assorting by materials that compose of the nano-platform, including iron-oxide-based nanoprobes, gadolinium-based nanoprobes, polymeric nanoprobes and other novel PET/MRI nanoprobes. By comparing the cons and pros of each probe, we also try to conclude the clinical demand for the design of PET/MRI probes and give some clues on the direction of further research on PET/MRI probes (**Scheme 1**).

2. Nano-Sized PET/MR Bifunctional Probes

2.1. Iron-Based Nanoparticles for PET/MR Imaging

The application of superparamagnetic iron oxide nanoparticles (SPION) such as Fe_3O_4 and γ-Fe_2O_3 in MRI imaging can be traced back to the 1990s.[13] Up to now, there are many Iron-based nanoparticles with a size ranging from 1 to 200 nm been applied as MRI contrasts, such as ferumoxytol and Resovist. Generally speaking, the large Iron oxide nanoparticles are preferred for T2 imaging, while the ones with smaller size are more suitable for T1 imaging.[14] Compared to traditional GBCA, the FeO_x nanoparticles have superior biosafety in patients with nephrogenic systemic fibrosis (NSF) and diseases in the central nervous system (CNS).[15] To prepare PET/MRI bifunctional probes, the FeO_x nanoparticle should be labeled with radioisotopes that are capable of PET imaging, such as ^{68}Ga, ^{64}Cu, and ^{18}F. Benefiting from the versatile surface functional properties of nanoparticles, different methods could be used to radiolabel the FeO nanoparticles. In this section, we would introduce FeO-based PET/MRI probes that radiolabeled with different radioisotopes.

^{68}Ga radiolabeled FeO_x nanoparticles

^{68}Ga is a commonly used radioisotope for PET imaging. It is usually produced by a Ge/Ga generator and has a half-life time of 68 min.[16] Compared to other PET radionuclides, the ^{68}Ga is more available for majority of hospitals, while only the hospitals own clinical cyclotrons can conveniently produce ^{18}F, ^{11}C and other high energy positron-emitting radioisotopes.[17] Moreover, unlike ^{14}C and ^{18}F which require relatively more complex radiolabeling, the radioactive metallic Gd^{3+} ions can be easily bonded to nanoparticles by the coordination with chelators.

Kim et al. prepared a ^{68}Ga radiolabeled iron oxide nanoparticles (IONP) as a dual-modality tumor-targeted PET/MRI probe. The Fe_3O_4 nanoparticles were first synthesized via the thermal decomposition reaction, then the surface of the obtained nanoparticles was decorated with a chelator, namely 1,4,7-triazacyclononane-1,4,7-triacetic acid (NOTA). Finally, ^{68}Ga ions were applied to radiolabel the Fe_3O_4 nanoparticles by coordinating with NOTA (**Figure 1**). The final product ^{68}Ga-NOTA-OA(oleanolic acid)-IONP exhibited excellent r2 relaxivities as well as good stability in both PBS buffer and serum. A 4.7T animal MRI and micro PET were then applied to visualize the lesion in tumor-bearing mice. It was found that the new probe does not only provided information on the tumor functionality and progression, but also enabled the accurate quantification of the tumor tissues.[18] Chelators play an important role on the ^{68}Ga radiolabeling. Besides NOTA, other chelators, such as dodecane tetraacetic acid (DOTA) and diethylenetriamine penta acetic acid (DTPA) could also be used for loading $^{68}Ga^{3+}$ ions on FeO_x nanoparticles.[19,20] For instance, Sattarzadeh et al. used DTPA ligand for bridging silica-coated Fe_3O_4 nanoparticles and ^{68}Ga. Then they applied PET/MRI technique to trace the biodistribution of the probes in healthy mice and found out that the gallium complex is highly stable in vivo.[20]

To modify the radiolabeling process of FeO_x-based PET/MRI probe, FeO_x nanoparticles with various functionalization were studied. One example is the polyethylene glycol (PEG) coated superparamagnetic iron oxide nanoparticles (SPION). The PEGylated SPIONs were found to directly react with ^{68}Ga ions

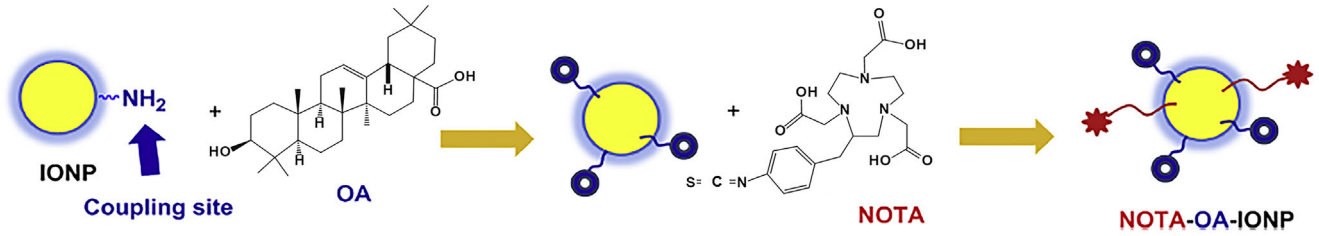

Figure 1. Schematic of the hybrid PET/MR imaging agent created with an oleanolic acid-conjugated nanoparticle. Adapted with permission.[18] Copyright 2013, Elsevier.

without any chelators, achieving high radiolabeling efficiency and high radiochemical stability.[21] PET/MRI was utilized to visualize the biodistribution of the probes in vivo and found that this probe is suitable for the diagnosis of malignancies in the liver and spleen. Apart from PEG, carboxydextran has also been utilized to functionalize FeO-based probes. To distinguish the metastatic sentinel lymph node (SLNs) from the healthy ones, Savolainen et. al. prepared carboxydextran coated SPIONs and used these particles as PET/MRI probes after being radiolabeled by ^{68}Ga (**Figure 2**). PET imaging can provide full-body imaging with high sensitivity, while MRI imaging are capable of evaluating intra-LN SPIONs distribution. Both PET and MRI indicated

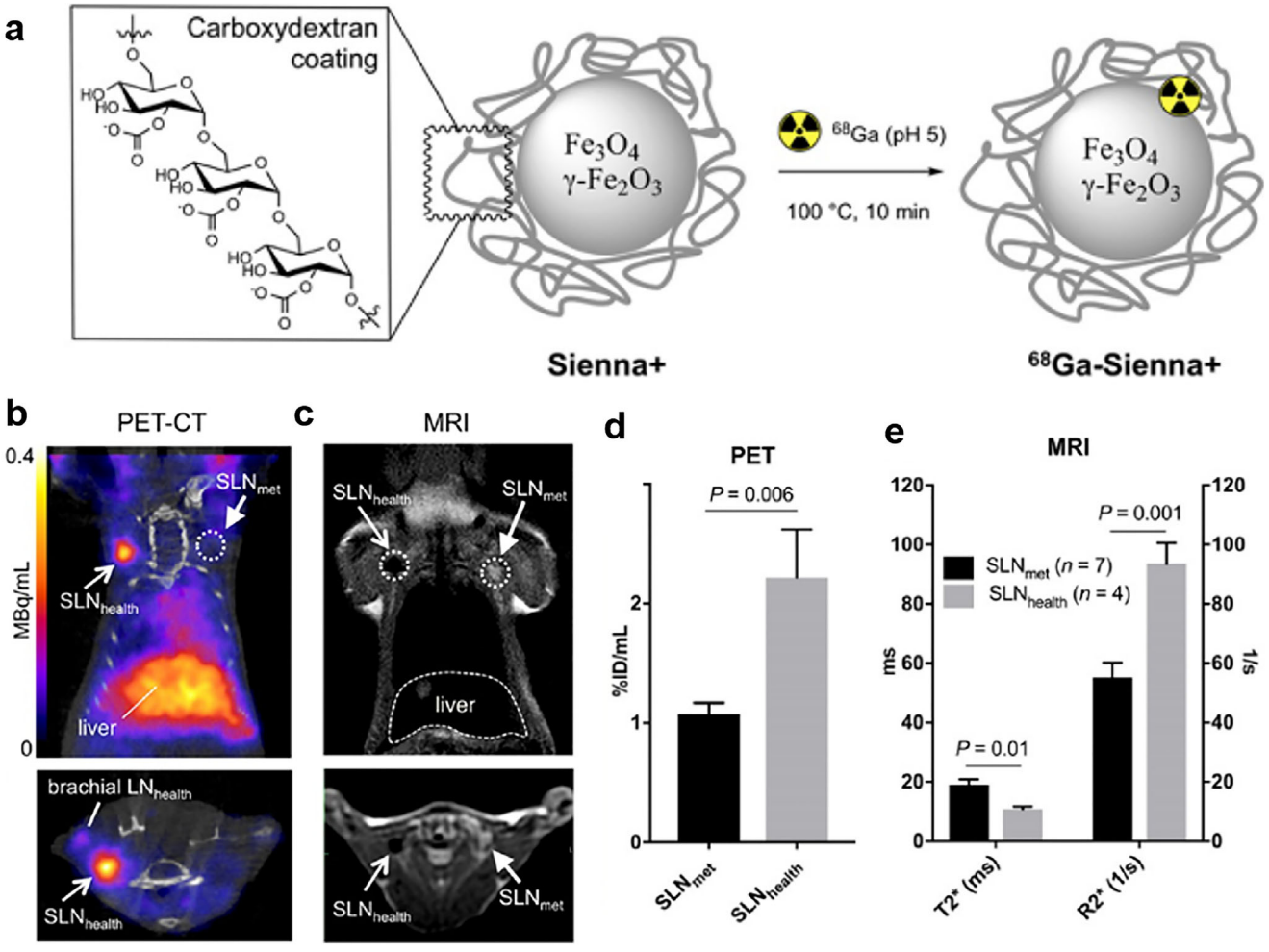

Figure 2. a) ^{68}Ga-radiolabelling of Sienna+; In vivo imaging in the 3E.Δ.NT metastatic breast cancer model: b) coronal and transversal PET-CT images for the mouse showing uptake of ^{68}Ga-Sienna+ in SLN health (open arrowhead), but not in SLN met. Note that, for clarity, the injection site and corresponding PET signal is not shown; c) coronal and transversal MRI images (T2-weighted 3D turbo spin echo) of the same mouse showing the uptake of 68Ga-Sienna+ in SLN health, but not in SLN met that appear bright and enlarged; ^{68}Ga-Sienna+ uptake quantification (mean ± SEM) in SLN met and SLN health by d) PET and e) MRI. Adapted with permission.[22] Copyright 2019, Ivyspring International Publisher.

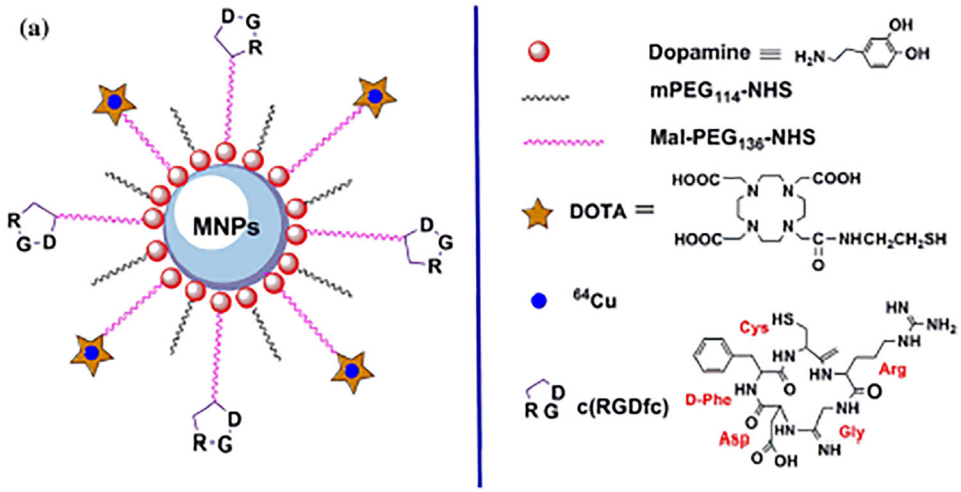

Figure 3. Illustration of tumor-targeting PET/MRI dual-modal imaging agent: ^{64}Cu-SPION-dopa-PEG-DOTA/RGD. Adapted with permission.[27] Coyright 2022, Springer Nature.

that the healthy SLN has higher uptake of the SPIONs than the metastatic counterpart, which allows this probe applicable for distinguish healthy and metastatic SLNs.[22] Moreover, other substances, such as dendrimers and alginate could also be used to coat SPIO nanoparticles for radiolabeling with ^{68}Ga and in this way acquiring PET/MRI images.[19,23]

Rather than only being applied as PET/MR imaging probes, the FeO_x nanoparticles with versatile properties have shown the potential for other clinical applications. A typical example is to use the FeO_x-based nanoplatform as theragnostic agents. Cho et al. prepared the folate-conjugated Fe_3O_4 nanoparticles that were loaded with the chemotherapeutic medicine doxorubicin (DOX), then radiolabeled the nano-complex with ^{68}Ga. This nanoplatform is capable of PET/MR imaging, as well as delivering the drugs for cancer treatment.[24] In another case, researchers used ^{68}Ga-SPIONs as a triple-modality imaging agent, saying PET, MRI and Cherenkov imaging. The Cherenkov luminescence is generated during the decay of ^{68}Ga, which could be detected by a slow-scan deep-cooled CCD camera. The triple modality probe was applied to identify the sentinel lymph node, both qualitatively and quantitatively.[25]

^{64}Cu radiolabeled FeO nanoparticles

^{64}Cu is another metallic positron emitter for PET imaging with a half-life of 12.7 h. Similar to ^{18}F, ^{64}Cu could be in-site produced by a hospital cyclotron, which however requires more power than the production of ^{18}F.[26] Considering its metallic nature, the ^{64}Cu can also be linked to nanoparticles by coordinating with chelators such as DOTA. Shi et al. prepared a PET/MRI dual-modal imaging probe by attaching ^{64}Cu to surface of the SPION nanoparticle modified by DOTA (**Figure 3**). By further modifying the nanoparticles with $\alpha_v\beta_3$ targeted peptide RGD(Arg-Cly-Asp), the probe exhibited high specific tumor targeting ability. Tumor-bearing mice with $\alpha_v\beta_3$ expression human glioblastoma xenograft were used as the animal model, a 7T small animal MRI and MicroPET were applied to visualize the in vivo behavior of the probes. The results demonstrated that this probe indeed has tumor-targeting property, therefore could be used as a potential tool for PET/MR imaging.[27]

The in vivo ion release of PET probes radiolabeled with metallic radioisotopes is crucial for nuclear medicine. The released metal ions might not only provide inaccurate disease information but also lead to radiation damage to the tissue where these ions accumulated. So far, the chelators are of great importance as the bridge between metallic radionuclide and the nanoparticles that waiting to be labeled. Apart from the commonly used chelators such as DOTA and NOTA, some new chelators with stronger coordination properties have also been applied for ^{64}Cu radiolabeling.[28] Thomas et al. developed a new macrocyclic chelator, namely MANOTA, for successful radiolabeling of the SPION NPs with ^{64}Cu. PET/MRI technique was applied to evaluate the in vivo stability of the new probe, Fe_3O_4-LDOPA-PEG-MANOTA-^{64}Cu. The highest signal of both MRI and PET were found at the liver where the nanoparticles mostly accumulated in the reticuloendothelial system, revealing that the bond between ^{64}Cu ions and Fe_3O_4 NPs is stable and no Cu^{2+} ions leakage occurred (**Figure 4**).[29] Some publications also point out that bisphosphonates and their derivatives can be used to connect ^{64}Cu and iron oxide nanoparticles, the obtained products exhibit pretty excellent radiolabeling stability and are suitable to be used as the novel PET/MRI probes.[30,31] Interestingly, researchers also developed a chelator-free method to radiolabel the iron oxide nanoparticles by adding radioactive Cu^{2+} ions into iron precursor solutions during the synthesis process.[32] Compared to the chelators coordinated radioisotopes which usually locate on the surface of iron oxide nanoparticles, the incorporated ones apparently have superior stability since the encapsulated Cu^{2+} ions have less chance to interact with serum and other substances in bloodstream.

Other radionuclide labeled FeO nanoparticles

^{18}F is the most popular PET radionuclide in the clinic. It has a half-life time of 110 min and can be in-site produced by hospital cyclotron. The suitable half-life allows ^{18}F-based PET probes have enough time for data acquisition without exposing the patients to ionizing radiation for a long period. However, the radiolabeling of ^{18}F is commonly achieved via substitution reaction with organic molecules, direct ^{18}F radiolabeling of nanoparticles is

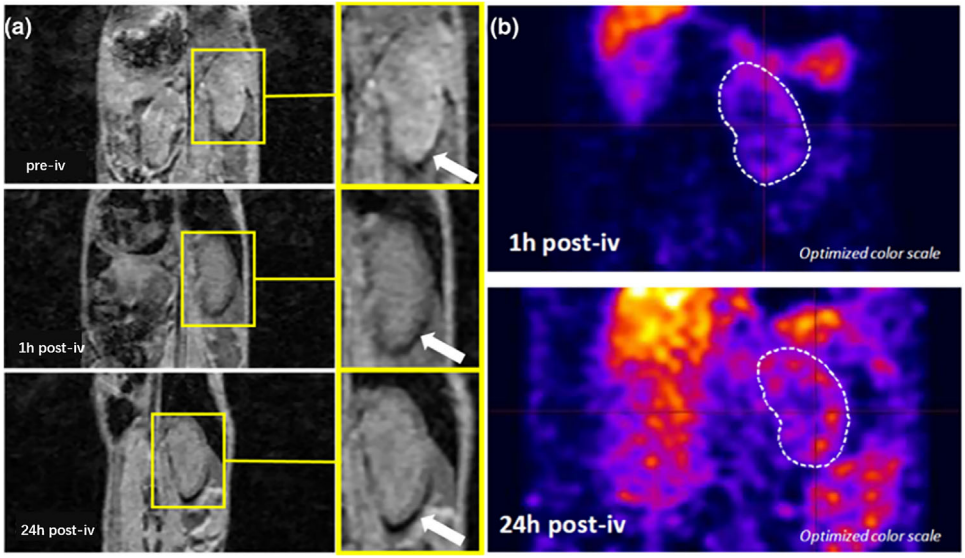

Figure 4. a) 3D T2*-weighted MR images and b) PET imaging of rena cortex at different time of injection: before injection (pre-iv) for MRI, after 1 h (1 h post-iv), and 24 h (24 post-iv) after injection of Fe_3O_4-LDOPA-PEG-MANOTA-^{64}Cu in a mouse. Adapted with permission.[29] Copyright 2019, American Chemical Society.

rarely seen for inorganic PET probes. Nevertheless, the ^{18}F show quite a strong affinity to certain metal ions, especially Al^{3+} ions, which leaves some potential for the ^{18}F labelling of nanomaterials. Sun et al. prepared a NOTA conjugated IONPs (NOTA-COBP-IONPs) as the nanoplatform for PET/MR imaging. By adding Al^{3+} ions and radioactive ^{18}F ions together to the IONPs solution, they eventually prepared the ^{18}F-AlF labeled NOTA-COBP-IONPs. Based on the results of animal imaging, they pointed out that the synergic information obtained from both PET and MRI can significantly improve the diagnosis accuracy.[33] Rather than applying the surficial chelator for coordinating with ^{18}F-AlF ions, Cui et al. directly coated the magnetic nanoparticles with an $Al(OH)_3$ layer, which could further be used to ^{18}F labeling.[31] The results prove that the complex made up with $Al(OH)_3$ coated iron oxide NPs and ^{18}F is stable under PBS and serum.

There are a few studies that use other isotopes to radiolabel iron oxide nanoparticles for fabricating PET/MR probes. Apart from the above-mentioned isotopes, ^{89}Zr is another promising candidate for PET imaging with a half-life of 3.3 days. Thorek et al. prepared ^{89}Zr radiolabeled iron oxide nanoparticles, that is, ^{89}Zr-ferumoxytol, for imaging of the lymphatic system (**Figure 5**). By using this as-obtained probe, PET/MRI can localize the draining lymphatics in both the axillary and the abdominal regions, which benefit for evaluating the lymphatic functions.[34] Cai's group developed a chelator-free method to label SPION with radioactive Arsenic($^{*}As^{III}$) which has four positron emitting isotopes, saying $^{70/71/72/74}$As. The arsenic element has a very strong affinity to magnetic materials, which would lead to a physical absorption of $^{*}As^{III}$ on the surface of SPION. According to the PET/MR imaging results, this probe exhibited quite excellent in vivo stability as well. Another interesting example is the one that combined ^{124}I with SPION for PET/MR imaging by iodination reaction. In this case, ^{124}I is not only a positron emitter but also can produce Cherenkov luminescence, which allows the novel PET/MRI probe to be used for optical imaging as well.[35]

2.2. Gadolinium-Based Nanoparticles for PET/MR Imaging

Gadolinium-based materials have been applied as enhanced MRI contrast for a long time. Gadolinium has seven unpaired electrons, which would lead to a shorten spin-lattice relaxation time (T1) and therefore result in brighter T1-weighted images.[36] Some Gd-based compounds, such as Gd-DTPA and Gd-DOTA, have shown quite good clinical outcome. However, these Gadolinium complexes have several drawbacks, such as in vivo destabilization and inadequate Gd relaxivity,[37] leading to Gd leakage and a higher Gd injection, respectively. Encapsulation of Ga ions inside a "cage," for instance, fullerene, would significantly improve the stability of Ga-based MRI probes.[38,39] Chen et al. developed a novel PET/MRI probe by labeling the alanine-modified gadofullerene nanoparticle, namely $Gd@C_{82}$, with ^{64}Cu or ^{89}Zr. Additionally, the RGD peptides were further utilized to improve the tumor targeting property. [40] They used tumor-bearing mice to evaluate the function of the novel PET/MRI probes. The MRI images give a very clear tumor boundary, while the PET images allow the quantitative analysis of the tumor uptake. The combination of PET and MRI provide more precise diagnosis results.

Another Gd-based material used for PET/MRI imaging is AGuIX nanoparticle, which is kind of chelate that composed of polysiloxane and gadolinium. AGuIX usually has a hydrodynamic diameter under 5 nm, which in theory have better tumor uptake due to the EPR (Enhanced Permeability and Retention) effect.[41] Tran et al. developed a novel PET/MRI probes by radiolabeling AGuIX nanoparticles with ^{64}Cu. By optimizing the macrocyclic chelating silane precursors and synthesis parameters, they eventually obtained the probe, namely SiGdNP@N-1, with good stability and PET/MR imaging properties.[42] 1 year later, Thakare et al. prepared the dual functionalized AGuIX nanoparticles decorated by macrocyclic chelator NODAGA and a near-infrared heptamethine cyanine dye, after being radiolabeled by PET

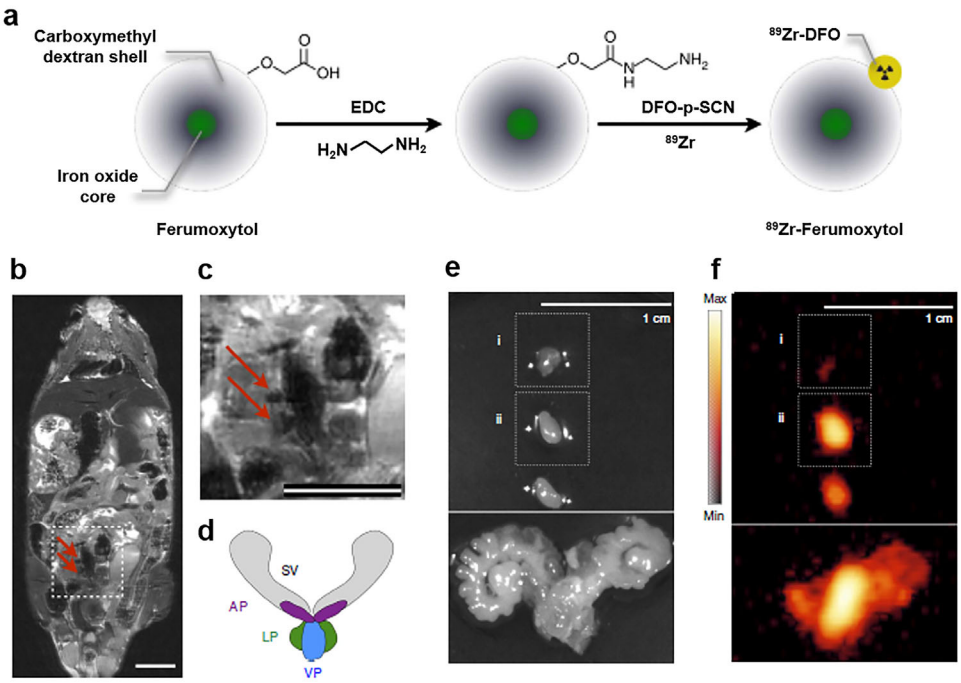

Figure 5. a) Schematic of the carboxyl-terminated polyglucose sorbitol carboxymethylether coating (grey) surrounding the iron oxide crystal core (green) of the nanoparticle. Amination of the particles was carried out before their functionalization with B7 DFO chelates. Intraprostatic administration reveals pelvic lymph node distribution for therapy planning and surgical confirmation. ^{89}Zr-ferumoxytol (5 mL, 35 mCi) was administered to the AP. Imaging was conducted B6 h after injection. b) The negative contrast produced by the nanoparticles is visible in a whole-body coronal MR slice (red arrows). c) On greater magnification of the coronal MR image, it is possible to distinguish two in-plane draining nodes from signal voids created by the nanoparticles (red arrows), however this task is difficult with MRI alone as there are other regions of low signal intensity. Scale bars on MR images are 0.8 cm. d) For reference to the following dissection, a schematic diagram of the mouse prostate organ is provided showing the SV, seminal vesicles; LP, lateral prostate; VP, ventral prostate and AP, anterior prostate. e) PET and MRI were used as preoperative planning tools for radical prostatectomy and LN dissection, by visual guidance. A white light macrograph of the excised tissues with 1 cm scale is shown. f) In order to verify that the targeted structures were indeed removed, ex vivo PET was performed. Intraoperatively, this role could be carried out with a handheld beta probe. The AP and two of the excised specimens were detected by PET. Adapted with permission.[34] Copyright 2014, Springer Nature.

radioisotope, ^{64}Cu or ^{68}Ga, this newly-developed nanoplatform was applied for PET/MRI/Optical tri-modality imaging.[43] As shown in **Figure 6**, PET/MRI images indicates that the as-prepared nanoprobes have evident accumulation at the tumor site, which shows it potential to be used as novel PET/MRI probe. Apart from pure imaging function, the AGuIX-based probes can provide more contribution to disease treatment. For instance, Justine et al. utilized ^{68}Ga-radiolabeled AGuIX nanoparticles as the PET/MRI probes to evaluate blood-brain barrier(BBB) injury caused by stroke.[44] Penelope et al. combined AGuIX nanoparticles which are sensitive to radiation and PET/MRI techniques to achieve imaging guided radiation therapy.[45]

2.3. Manganese-Based Nanoparticles for PET/MR Imaging

Manganese has also been studied as the MRI contrast for a long time. This element has 5 unpaired electrons, slow electron relaxation and fast water exchange rate, which so far makes it attractive for T1 MR imaging.[46] Quite a few Mn-based MRI contrast reagents have been developed, such as Mn-containing small molecular compounds, Mn-containing polymers and Manganese oxide nanoparticles.[47,48] As a popular MR imaging reagent, MnO_x nanoparticles have been explored for the possibility as PET/MRI dual imaging probes.[49] Zhu et al. prepared a novel PET/MRI probe composed of polyethyleneimine-coated Mn_3O_4 nanoparticles and ^{64}Cu radioisotope. NOTA ligand works as the chelators for the connection of radioactive Cu^{2+} and Mn_3O_4 nanoparticles. To improve the tumor-targeting property, folic acid (FA) has been conjugated on the surface of Mn_3O_4 nanoparticles.[50] The as-prepared PET/MRI probe was tested to visualize the mouse xenografted with human cervical cancer that overexpress folate receptors. The results turned out that the as-prepared MnOx-based dual imaging probe had specific targeting ability to the tumor lesion and could quantitatively measure the folate receptor at the tumor sites

Similarly, Zhan et al. also prepared Mn_3O_4 nanoparticles that combined with ^{64}Cu for PET/MRI dual imaging. Rather than the small molecular targeting reagent, they utilized the anti-CD105 antibody TRC 105 that specifically targeted to tumor vasculature to enhance the targeting property of the as-obtained probes. The PET/MR images clearly revealed the biodistribution of the new probes and demonstrated that the probe has neglected long-term toxicity to mice.[51] Another example that applying MnO_x nanoparticles as PET/MR dual-modality imaging has been carried out by the same group. In this work, instead of using chelators to bind MnO_x NPs and metallic radioisotopes, they used a chelator-free method to prepare ^{89}Zr labeled MnO_x

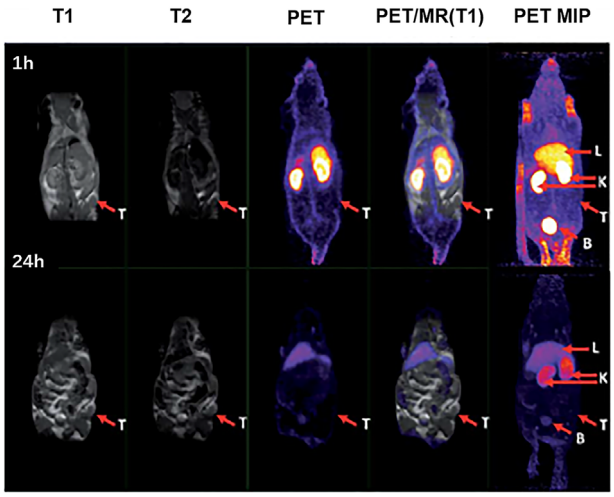

Figure 6. (C) PET-MRI images 1 h (top) and 24 h (bottom) post injection (T ¼ tumor, K ¼ kidneys, B ¼ bladder and L ¼ liver). MIP stands for Maximum Intensity Projection. Adapted with permission.[43]Copyright 2019, Royal Society of Chemistry.

nanoparticles which making use of the high affinity between Zr^{4+} ions and manganese oxide nanoparticles. The PET/MR image result shown in **Figure 7** clearly demonstrated that the nanoprobes have a primary accumulation at lymph nodes, which so far could be used for lymph node mapping.[52]

2.4. Soft Nanoparticle for PET/MR Imaging

Polymeric nanoparticles such as polymersomes, micelles and dendrimers have been widely applied for disease diagnosis and treatment. The soft nature of these polymeric nanoparticles allows them to be diversely functionalized and thus to interact with many clinical reagents. The easiest approach to prepare soft PET/MRI probes is to merge the clinical MR contrast reagent and PET probes into one polymeric nanoplatform. For instance, Vecchione et al. fabricated a typical soft nanoplatform composed of a chitosan core and a hyaluronic acid shell. By entrapping ^{18}F-FDG and Gd-DTPA into the nanoparticles, they successfully prepared a novel dual-modality probe and carried out simultaneous PET/MRI data acquisition on a homemade body phantom.[53] The results indicate that the nanoplatform is capable of boosting the relaxometric properties and thus result in five times enhancement of r1 than the pure Gd-DTPA. Another interesting example is to graft Fe^{3+}-deferoxamin (Fe-DFO) and ^{89}Zr-deferoxamin (^{89}Zr-DFO) onto the surface of micelles that are composed by PBD-b-PEO and PBD-b-PAA for PET/MRI dual-modality imaging. Benefiting from the EPR effect of micelles, the PET/MRI probe shows evident accumulation at tumor sites, and thus yields high tumor-to-blood and tumor-to-muscle ratios, further leading to better image quality.[54]

Other novel polymeric nanoparticle-based PET/MRI probes have also been explored. Xia et al. constructed organic melanin nanoparticles that containing Mn^{2+} ions and ^{124}I as the multimodality imaging probes (**Figure 8**). Additionally, the melanin nanoparticles themselves could be used for photoacoustic imaging (PAI), so far the new probe is a multimodality probe that could be used for PET/MR/PAI imaging. By coating the melanin nanoparticles with somatostatin analog octreotide, they used the newly-developed probes for targeted imaging of human small-cell lung cancer (SCLC). The PET/MR/PAI imaging results indicate that the nanoprobes have very high targeting properties of the NCI-H69 tumor model that has a high expression of somatostatin receptor subtype 2.[55] A similar work was carried out by the same group. Other than SCLC targeted probe, they prepared a prostate cancer targeted nanoplatform by linking a prostate-specific membrane antigen (PSMA) inhibitor, PSMA-SH on the surface of the probes. After loading the melanin nanoparticles with ^{89}Zr and Mn^{2+} ions, they applied PET/MRI to visualize the in vivo biodistribution of the probe and evaluate the therapeutic outcome on prostate cancer. The application of the dual imaging probes can help to figure out the accurate location of tumor and display the tumor volume in real-time, which therefore would lead to better therapeutic outcome.[56]

Some novel method has been developed for preparing PET/MRI dual imaging probes that made of soft materials. For instance, Li et al. developed a smart nanoplatform based on nanoporphyrin. The presence of porphyrin allows the nanomedicine to load ^{64}Cu and Gd^{3+} together, which in this way provides PET/MR imaging property. Besides, the core of this nanomedicine could be used to encapsulate therapeutic reagents, such as Doxorubicin and fluorescent substance, which allows this nanoplatform to have versatile functions.[57] Interestingly, Aryal and his colleagues designed a modified nanoprecipitation method to prepare PET/MRI nanoprobes. They mixed poly (lactic-*co*-glycolic acid) (PLGA), lipids and polyethylene glycol (PEG) together with iron oxide nanoparticles which has a size of 5 nm, followed by radiolabeling the nano products with ^{64}Cu, thus forming the PET/MRI probe, namely PEMs.[58] The long circulation period and EPR effect of nanomedicine allow the visualization of this probe and tumor lesion in a long term over multiple scales, which makes the nanoplatform be potential for clinical translation.

In the above-mentioned examples using soft nanoparticles (SNs) for PET/MR imaging, both PET isotopes and MRI contrast enhancers are presented in one vector. However, some soft material-based probes that do not contain MRI contrast reagents could be applicable for PET/MR imaging as well. In these cases, the application of MR imaging is aimed at achieving better structural information on the disease lesions without any assistant from contrast enhancer. As one of the most applied isotopes, ^{18}F shows its potential on being radiolabeled on these soft nanoparticles. Nagachinta et al. applied ^{18}F to radiolabel an organic lipid-based nanoprobe, and then used PET/MR technique to trace the in vivo biodistribution. Instead of directly labeling ^{18}F to the nanoprobes, a ^{18}F-contained small molecule, saying [^{18}F]FBEM was first synthesized, which can be used to interact with the nano-vectors (**Figure 9**). The PET/MR images demonstrated that the probe mainly accumulates at the liver and spleen, the radiochemical stability of this probe was high and no evident ^{18}F leakage was observed.[59] Recently, Vaughan et al. prepared a novel polymeric particle composed of poly(beta-amino-ester) to deliver DNA for the gene therapy of hepatocellular carcinoma. To trace the DNA-containing vector and evaluate its tumor killing performance, they used ^{18}F containing small molecule, 9-(4-^{18}F-fluoro-3-hydroxymethylbutyl) guanine (^{18}F-FHBG), to radiolabel

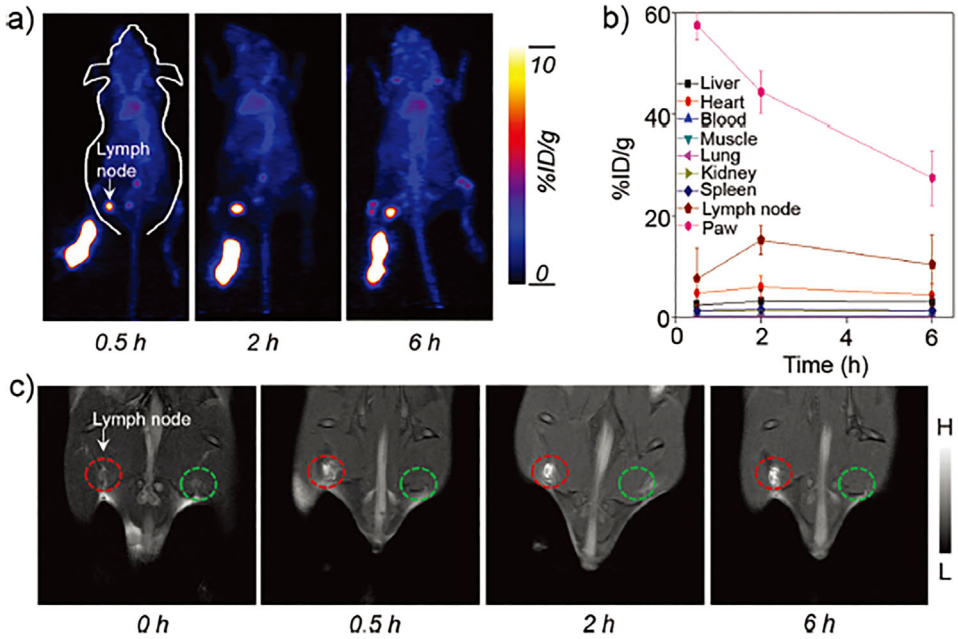

Figure 7. In vivo PET/MR imaging of lymph nodes with [^{89}Zr]Mn_3O_4@PEG NPs. a) In vivo PET imaging acquired after subcutaneous injection of [^{89}Zr]Mn_3O_4@PEG NPs into the left footpad of the mouse ($n = 3$). Lymph nodes are indicated by arrows. (=b) Quantification of the [^{89}Zr]Mn_3O_4@PEG NPs uptake by the lymph node, paw, heart, liver, kidney, blood, lung, muscle and spleen ($n = 3$). c) In vivo MR imaging of the lymph nodes before and after injection of Mn_3O_4@PEG NPs into the left footpad of the mouse ($n = 3$). Lymph nodes are indicated by circles. Adapted with permission.[52] Coyright 2019, American Scientific Publishers.

the nano vector. The MR images demonstrate that the tumor area was reduced after being treated by gene therapy, which is further verified by the quantitative measurement of PET imaging with less activity uptake has been found in the tumor site for the treatment group.[60]

The combination of PET/MRI techniques and soft nanoparticle-based probes has a broad application in the diagnosis of various diseases. For instance, to better visualize the atherosclerotic vessel wall, Lobatto et al. prepared ^{89}Zr-labeled liposomes as a multimodal imaging probe. PET/MRI technique was employed to study the biodistribution of the radioactive liposomes in animal model. The results pointed out that the probes can be quickly excreted by healthy animals, and no evident radioactive spot could be found on the third day post-administration. While distinct radiation spots could be observed in the atherosclerotic animals. Benefited from the T_2-weighted MR image, they successfully colocalized the nanoprobes within the thickened vessel wall.[61] KÖRHEGYI et al. synthesized a nanoplatform composed with PGA(Poly-gamma-glutamic acid) and chitosan decorated with folic acid that specifically targeted

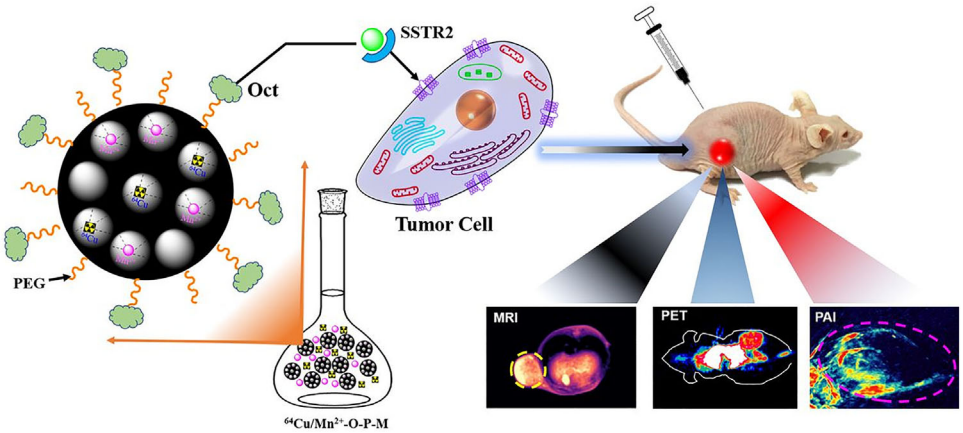

Figure 8. Synthesis and characterization of (^{124}I, Mn)-OCT-PEG-MNPs. OCT-PEG-MNPs can specifically bind to the surface receptors of $SSTR_2$ highly expressed tumor cells. ^{124}I and Mn^{2+} were used to construct a tumor targeting nanoprobe for MRI/PET/PAI multimodal imaging of human small cell lung cancer. Adapted with permission.[55] Copyright 2019, Royal Society of Chemistry.

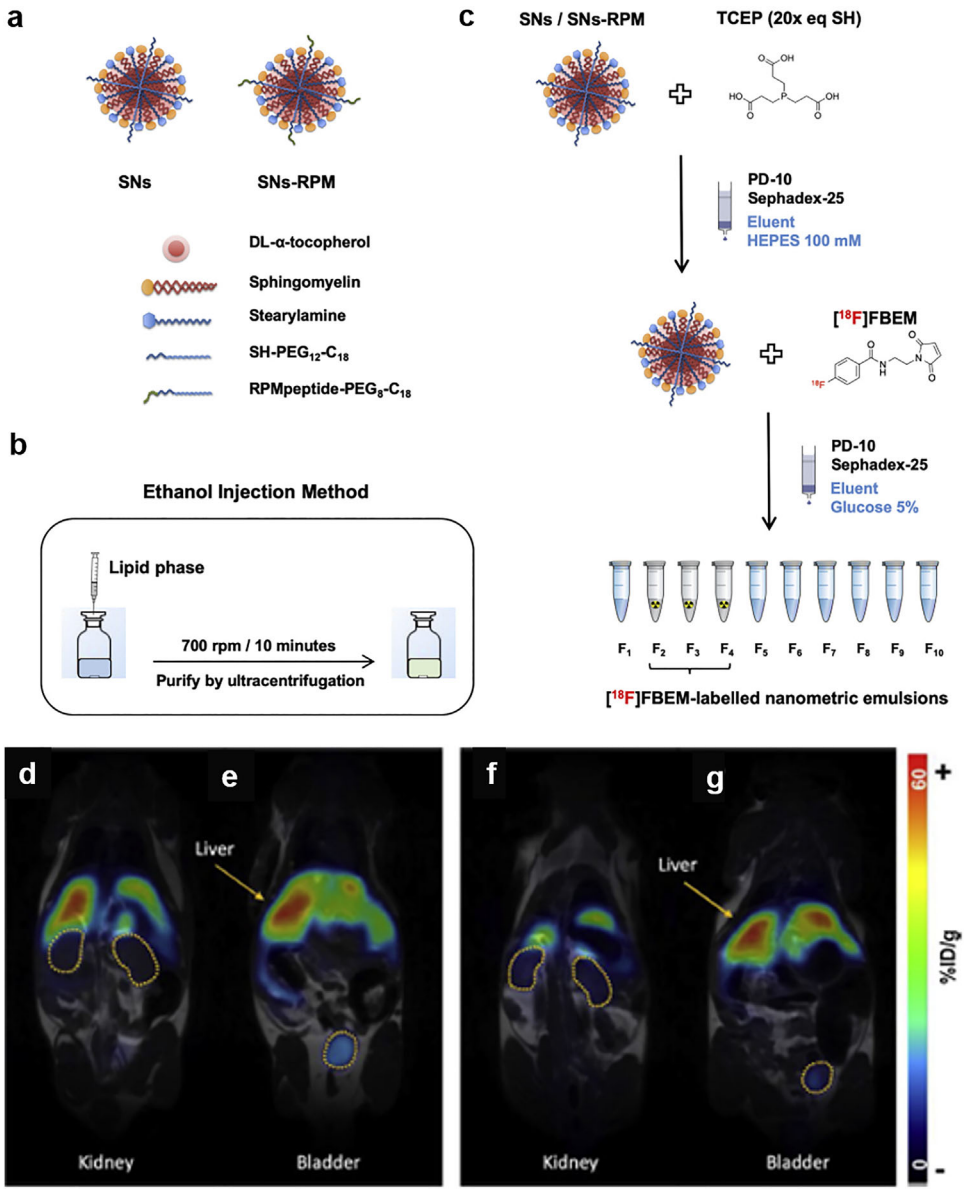

Figure 9. a) Components and Scheme of preparation of SNs and SNs-RPM; b) Radiolabeling steps of SNs-[^{18}F]FBEM and SNs-RPM-[^{18}F]FBEM; c) Whole body in vivo biodistribution of SNs-[^{18}F]FBEM (left) and SNs-RPM-[^{18}F]FBEM (right) in BALB/c mice 2 h p.i. using PET and MRI: two different coronal slides showing respectively the d,e) kidney and the f,g) liver and bladder. Adapted with permission.[59] Copyright 2020, Elsevier B.V.

KB human cervical carcinoma cells. A modified NODAGA chelator was applied to coordinate the nanoplatform with ^{68}Ga. To evaluate the targeting property of the as-prepared nanocarriers, they applied PET/MRI technique to observe the biodistribution of the nanoplatform. The images indicate that the presence of folic acid would indeed improve the accumulation of probes in the mice that planted with folic acid overexpression cell line.[62]

2.5. Other Particles for PET/MR Imaging

Apart from the above-mentioned nanoparticles that have been studied for PET/MRI dual-modality imaging, other probes, such as $MnFe_2O_4$ and Au nanoparticles also show their potential in PET/MR imaging. Superparamagnetic manganese ferrite ($MnFe_2O_4$) nanoparticles exhibit superior MR imaging performance due to their high magnetization and larger relaxivity. For instance, Choi et al. fabricated a $MnFe_2O_4$ nanoparticles-based PET/MRI probe for visualizing the lymph node (LN). Considering the LN mapping is strict on the probe morphology, the hydrodynamic size of the $MnFe_2O_4$ nanoparticles is controlled within 40 nm. Radioisotope ^{124}I was used for PET imaging in this work. With the help of this novel probe, they accurately distinguished the axillary LN and brachial LN by PET/MR imaging (**Figure 10**).[63] Shi et al. prepared the RGD-modified $MnFe_2O_4$ nanoparticles as the platform. To prolong the in vivo circulation, they modified the surface of $MnFe_2O_4$ nanoparticles by PEG-dopa. Meanwhile, they decorated the surface of the nanoparticles

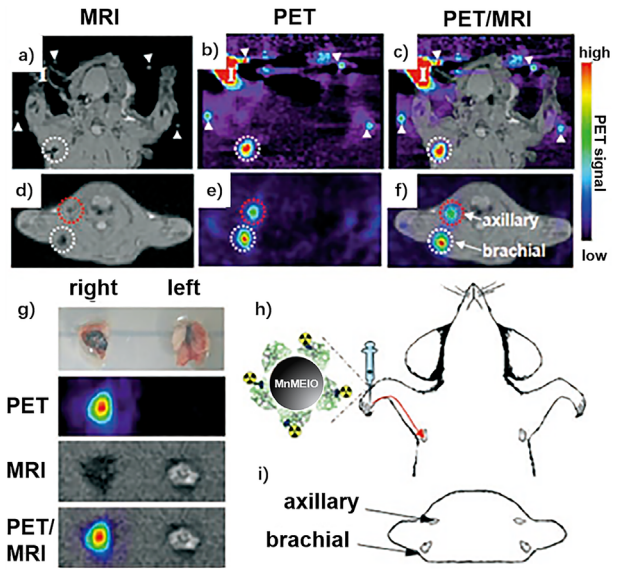

Figure 10. a–f) PET/MR images of SLNs in a rat at 1 h post injection of ^{124}I-SA-MnMEIO into the right forepaw (I = nanoprobe injection site). Coronal a) MR and b) PET images in which a brachial LN (white circle) is detected. c) The position of the brachial LN is well matched in a PET/MR fusion image. Four small pipette tips containing Na^{124}I solution are used as a fiducial marker (white arrowheads) for the concordant alignment in PET/MR images. In the transverse images, axillary (red circle) and brachial LNs (white circle) are detected in the d) MR and e) PET images, and images of each node are nicely overlapped in the corresponding f) PET/MR fusion image. g) The explanted brachial LN also shows consistent results with in vivo images by PET and MR. Only the LN from the right-hand side of the rat containing ^{124}I-SA(serum albumin)-MnMEIO shows strong PET and dark MR images. The schematics of the rat in the h) coronal and i) transverse directions show the locations of the LNs. Adapted with permission.[63] Copyright 2008, WILEY.

with DOTA derivative which could be further used to coordinate with ^{64}Cu. The MR images indicated that the nanoparticles with RGD modification showed better tumor accumulation than the ones without the target reagent. Additionally, the PET images demonstrated that the activity accumulated at the tumor sites of mice that were injected with RGD-conjugated $MnFe_2O_4$ nanoparticles was much higher, saying more than four times, compared to the mice that administrated nanoparticles without targeting modification.[64]

An interesting gold-iron oxide hetero-nanostructure, namely Au-Fe_3O_4 dumbbell-like NPs, has been fabricated by Cheng's group. NOTA was selected for radiolabeling with ^{64}Cu, and epidermal growth factor receptor (EGFR) targeted affibody was decorated on this hetero-nanoprobe. The fancy nanoplatform could be applied for PET/MR/Optical trimodal imaging. PET and MRI techniques were applied to observe the in vivo behaviors of the as-prepared probes, and both of them verified that the nanoprobes appeared at the tumor sites after 4h post-injection.[65] Another gold nanoparticle-based PET/MRI probe has been developed by Sun et al. In this case, they fabricated a melanin-coated gold nanorod as the platform that was capable of interacting with ^{64}Cu ions and Gd^{3+} ions in the absence of any chelator. Besides its function as a basic nanoplatform, the gold nanorod also plays the role of photoacoustic imaging reagent and photothermal therapeutic reagent. The as-prepared nanomedicine was utilized for the diagnosis and treatment of laryngeal cancer, which gained excellent therapeutic outcomes.[66] A similar work was carried out by Fortin et al. Rather than using gold nanoparticles, mesoporous silica nanoparticles (MSNs) that conjugated by DTPA chelator were prepared to incorporate ^{64}Cu ions and Gd^{3+} ions as PET/MR imaging reporters. The MRI results proved that the MSNs-based probe has better imaging properties than the Gd^{3+}-DTPA small molecules. Meanwhile, the PET figures revealed that the nanoprobe mainly accumulated at the liver, spleen and gastrointestinal system.[67]

Interestingly, some nanoprobes with complex composition have also been proven to be applicable as PET/MRI dual model reporters. Kandanapitiye et al. developed a novel $K^{68}Ga_xFe_{1-x}[Fe(CN)_6]$ nanoparticles by replacing the Fe^{3+} ions in Prussian blue (PB) with radioactive Ga^{3+} ions. The as-prepared nanoparticles show excellent paramagnetic properties with r1 and r2 value of 0.43 and 0.77 $mM^{-1}s^{-1}$ under a magnetic field of 1.4 Tesla, which is better than the clinical MR contrast reagent.[68] Moreover, the presence of radioactive ^{68}Ga allows the nanoparticles to be used for PET/MRI imaging. Luo et al. prepared a ^{124}I radiolabeled tri-gadolinium endohedral metallofullerene $Gd_3N@C_{80}$ as the PET/MRI dual-modality probes. To ensure the stability of the obtained Gd-containing nanoparticles, a fullerene was applied as cage that protects Gd^{3+} ions from leakage. Meanwhile, for successful ^{124}I radiolabeling, they used hydroxyl and carboxyl that can be iodinated to functionalize the surface of the $Gd_3N@C_{80}$. They first applied the MR technique to observe the location of the brain tumor in a rat. Both T1WI and T2WI indicated that the presence of $Gd_3N@C_{80}$ can strengthen the contrast of tumor lesions compared with normal tissue. Later on, a microPET facility was also applied to further confirm the intratumoral distribution of the PET/MR probes.[39] A PET/MR/Optical tri-modality probe has been developed by using ^{18}F-labeled $Gd^{3+}/Yb^{3+}/Er^{3+}$ co-doped $NaYF_4$ nanophosphors (NPs). In this system, Gd^{3+} ions can provide T1W MR imaging, ^{18}F is used for PET imaging, while the lanthanide ions co-doped nanoparticles could be applied to achieve upconversion luminescence. This multifunctional probe and its easy synthesis process might open new opportunities for the application of multimodal bioimaging techniques.[69]

3. Limitations and Perspective

Multi-modality imaging is gaining increasing attention in the clinic. The combination of different imaging techniques can overcome the shortage of the single ones and therefore provide greater value in disease diagnosis or even imaging-guided treatment. The MR is well-known for the high resolution of tissues, which shows its superior ability in the visualization of abnormality in vascular structure and neuro systems. PET imaging is quite a sensitive approach to evaluating the functions of certain organs or lesions. The combination of PET and MR would no doubt improve the diagnosis accuracy of various diseases. The dual-modality imaging probes are in this way required to achieve high quality images. The development of nanotechnology boosts the development of PET/MRI dual-modality probes. In this review, the novel PET/MRI probes have been comprehensively introduced according to the materials that are composed

of the nanoplatform, including the popular ones, for example, Fe and Gd-containing nanoprobes, and rare probes such as the ones based on gold or un-conversion materials. Though widely studied, there are still some limitations which humble the clinical translation of these PET/MRI probes.

The primary issue is the stability of the PET/MRI probe. To combine MR contrast reagent and PET reporter, generally, a nanoplatform is fabricated by magnetic nanoparticles, while the PET radioisotopes are grafted on the surface of the nanoparticles, chemically or physically. However, considering the complicated environment in vivo, for instance the proteins in bloodstream, the radioactive ions leakage is very likely to happen, which would lead to higher background noise or unexpected hot spots due to radioisotope accumulation. There are several approaches to conquering this dilemma, the most promising option is to choose a proper chelator with strong coordination ability with the isotopes. For instance, apart from these popular chelators such as DTPA, DOTA and NOTA, newly developed chelators, for example, bis(2-hydroxybenzyl)ethylenediaminediacetic acid (HBED) and tris(hydroxypyridinone) containing three 1,6-dimethyl-3-hydroxypyridin-4-one groups (THP), also show their potential in coordinating with metallic radioisotopes.[70,71] Another approach to prepare a probe with better in vivo stability is to entrap both PET reporter and MRI contrast with a proper cage. After being encapsulated into a cage, the ions have less chance to contact the serum and bloodstream, which would in theory lead to less leakage. However, the choice of the cage material has to be carefully considered.

Another problem that is required to be addressed before the clinical translation of the probe is the possible side-effect. The in vivo behaviors of nanoparticles are highly influenced by several aspects such as morphology, surface property and materials. Generally speaking, the particles with a hydrodynamic size range from 10 to 100 nm are very likely to end up in the liver and spleen, while the ones smaller than 6 nm would be easier to be excreted through the urinal system.[72–74] Though the nano-sized particles are supposed to be benefited from the EPR effects, the ERP effect differs a lot from patients and tumor types. The targeting modification is of great importance both for safety considerations and qualified imaging. In the above-mentioned examples, various targeting reagents have been applied, including small molecules., that is, folic acid and peptides such as RGD and PSMA-specific antibody. Therefore, a rational design with comprehensive consideration of both the physicochemical and biological properties of the nanoprobe is required to prepare a property PET/MRI probe.

The approvement by authorities is one of the biggest obstacles for the clinical translation of the PET/MRI probes. Though various novel nanomaterials have been explored for clinical application, only a few candidates have been approved. The Good Manufacturing Practices (GMP) of nanomaterials is still a big concern for the application of nanomedicine. As for the PET/MRI dual-modality probes, currently, there is still a blank in this field. A relatively easier way is to start with the already approved nanomedicines, such as USPIO and liposomes. However, it is still a big question for the approvement of new products that simply integrate two components that have already been approved. The mismatched properties would also reach a difficult situation. Therefore, more comprehensive and strict preclinical evaluation are still highly needed. As a relatively novel technique, the standard evaluation criteria for PET/MRI probes need to be figured out by clinical experts from both the imaging field and the medical field.

4. Conclusion

To sum up, we have reviewed the development of novel PET/MR dual-modality imaging probes by categorizing these probes with different compositions. The ones that are based on paramagnetic iron oxide nanoparticles, Gd-containing nanoparticles and soft nanoparticles are widely studied, while some nanoparticles composed by novel materials also show its potential as PET/MRI dual-modality probe. Due to the nature of nanomaterials, these probes could be given more functions such as optical imaging property and therapeutic properties. The underlying idea for the design of PET/MR probes is to radiolabel the existing MR components or encapsulate both PET isotopes and MR contrast reagents into a well-designed system. However, to achieve a PET/MRI probe that could be applicable in clinical, some obstacles still have to be conquered: a) the in vivo stability of the PET/MRI probes, saying that ions leakage has to be avoided as much as possible; b) the side effects such as background noise and possible harm to healthy tissue should be decreased by means of targeting treatment or proper medicine administration strategies; c) the materials of the probes should be considered, though some novel materials showed superior diagnose outcome, the real clinic approvement still needs a lot of effort. By summarizing the current research stage, this review hopes to point out the further direction of the development of PET/MRI probes and facilitate the clinical translation of dual-modality probes.

Acknowledgements

This research was supported by Medical Science and Technology Research Project of Henan Province (SBGJ202101002), Natural Science Foundation of Henan Province, China (222300420354, 212300410240).

Conflict of Interest

The authors declare no conflict of interest.

Keywords

dual-modality imaging, MRI, nanoprobes, PET, radiolabeling

Received: June 29, 2023
Revised: September 26, 2023
Published online:

[1] S. Siddique, J. C. L. Chow, *Nanomaterials (Basel)* **2020**, *10*, 1700.
[2] A. Lahooti, S. Sarkar, S. Laurent, S. Shanehsazzadeh, *Contrast Media Mol. Imaging* **2016**, *11*, 428.
[3] J. Lamb, J. P. Holland, *J. Nucl. Med.* **2018**, *59*, 382.
[4] G. Delso, S. Fürst, B. Jakoby, R. Ladebeck, C. Ganter, S. G. Nekolla, M. Schwaiger, S. I. Ziegler, *J. Nucl. Med.* **2011**, *52*, 1914.

[5] A. Kastelik-Hryniewiecka, P. Jewula, K. Bakalorz, G. Kramer-Marek, N. Kuznik, *Int. J. Nanomedicine.* **2021**, *16*, 8465.
[6] R. A. Cloyd, S. A. Koren, J. F. Abisambra, *Front Aging Neurosci* **2018**, *10*, 403.
[7] S. Tocchio, B. Kline-Fath, E. Kanal, V. J. Schmithorst, A. Panigrahy, *Semin Perinatol* **2015**, *39*, 73.
[8] E. Forte, D. Fiorenza, E. Torino, A. Costagliola di Polidoro, C. Cavaliere, P. A. Netti, M. Salvatore, M. Aiello, *J. Clin. Med.* **2019**, *9*, 89.
[9] M. N. Hood, A. D. Blankholm, A. Stolpen, *J. Radiol. Nurs.* **2019**, *38*, 38.
[10] G. Poletto, L. Evangelista, F. Venturini, F. Gramegna, F. Seno, S. Moro, R. Vettor, N. Realdon, D. Cecchin, *Pharmaceutics* **2022**, *14*, 2024.
[11] V. J. X. Phua, C. T. Yang, B. Xia, S. X. Yan, J. Liu, S. E. Aw, T. He, D. C. E. Ng, *Nanomater., (Basel)* **2022**, *12*, 582.
[12] L. R. Drake, A. T. Hillmer, Z. Cai, *Molecules* **2020**, *25*, 568.
[13] J. S. Weinstein, C. G. Varallyay, E. Dosa, S. Gahramanov, B. Hamilton, W. D. Rooney, L. L. Muldoon, E. A. Neuwelt, *J. Cereb. Blood Flow Metab.* **2010**, *30*, 15.
[14] H. Wei, O. T. Bruns, M. G. Kaul, E. C. Hansen, M. Barch, A. Wisniowska, O. Chen, Y. Chen, N. Li, S. Okada, J. M. Cordero, M. Heine, C. T. Farrar, D. M. Montana, G. Adam, H. Ittrich, A. Jasanoff, P. Nielsen, M. G. Bawendi, *Proc. Natl. Acad. Sci. U. S. A.* **2017**, *114*, 2325.
[15] E. A. Neuwelt, B. E. Hamilton, C. G. Varallyay, W. R. Rooney, R. D. Edelman, P. M. Jacobs, S. G. Watnick, *Kidney Int.* **2009**, *75*, 465.
[16] L. Martiniova, L. De Palatis, E. Etchebehere, G. Ravizzini, *Curr. Radiopharm.* **2016**, *9*, 187.
[17] F. Rösch, *Appl. Radiat. Isot.* **2013**, *76*, 24.
[18] S.-M. Kim, M. K. Chae, M. S. Yim, I. H. Jeong, J. Cho, C. Lee, E. K. Ryu, *Biomaterials* **2013**, *34*, 8114.
[19] T. Almasi, N. Gholipour, M. Akhlaghi, A. Mokhtari Kheirabadi, S. M. Mazidi, S. H. Hosseini, P. Geramifar, D. Beiki, N. Rostampour, D. Shahbazi Gahrouei, *Int. J. Polym. Mater. Polym. Biomater.* **2020**, *70*, 1077.
[20] E. Sattarzadeh, M. M. Amini, S. Kakaei, A. Khanchi, *J. Radioanal. Nucl. Chem.* **2018**, *317*, 1333.
[21] A. Lahooti, S. Sarkar, H. Saligheh Rad, A. Gholami, S. Nosrati, R. N. Muller, S. Laurent, C. Grüttner, P. Geramifar, H. Yousefnia, M. Mazidi, S. Shanehsazzadeh, *J. Radioanal. Nucl. Chem.* **2016**, *311*, 769.
[22] H. Savolainen, A. Volpe, A. Phinikaridou, M. Douek, G. Fruhwirth, R. T. M. De Rosales, *Nanotheranostics* **2019**, *3*, 255.
[23] E. A. Salvanou, A. Kolokithas-Ntoukas, C. Liolios, S. Xanthopoulos, M. Paravatou-Petsotas, C. Tsoukalas, K. Avgoustakis, P. Bouziotis, *Nanomaterials (Basel)* **2022**, *12*, 2490.
[24] B.-B. Cho, M. M. Moon, J. R. Chellan, S. H. Hwang, J. H. Lee, S. J. Jung, B. C. Kim, K. H. Yu, *Bull. Korean Chem. Soc.* **2016**, *37*, 886.
[25] T. A. T. Renata Madru, J. Axelsson, C. Ingvar, A. Bibic, *Am. J. Nucl. Med. Mol. Imaging* **2014**, *4*, 60.
[26] M. Jauregui-Osoro, S. De Robertis, P. Halsted, S.-M. Gould, Z. Yu, R. L. Paul, P. K. Marsden, A. D. Gee, A. Fenwick, P. J. Blower, *Nucl. Med. Commun.* **2021**, *42*, 1024.
[27] X. Shi, Y. Sun, L. Shen, *J. Radioanal. Nucl. Chem.* **2022**, *331*, 3485.
[28] M. Tosato, M. Verona, C. Favaretto, M. Pometti, G. Zanoni, F. Scopelliti, F. P. Cammarata, L. Morselli, Z. Talip, N. P. van der Meulen, V. Di Marco, M. Asti, *Molecules* **2022**, *27*, 4158.
[29] G. Thomas, J. Boudon, L. Maurizi, M. Moreau, P. Walker, I. Severin, A. Oudot, C. Goze, S. Poty, J.-M. Vrigneaud, F. Demoisson, F. Denat, F. Brunotte, N. Millot, *ACS Omega* **2019**, *4*, 2637.
[30] R. Torres Martin De Rosales, R. Tavaré, R. L. Paul, M. Jauregui-Osoro, A. Protti, A. Glaria, G. Varma, I. Szanda, P. J. Blower, *Angew. Chem. Int. Ed. Engl.* **2011**, *50*, 5509.
[31] X. Cui, S. Belo, D. Krüger, Y. Yan, R. T. M. De Rosales, M. Jauregui-Osoro, H. Ye, S. Su, D. Mathe, N. Kovács, I. Horváth, M. Semjeni, K. Sunassee, K. Szigeti, M. A. Green, P. J. Blower, *Biomaterials* **2014**, *35*, 5840.
[32] H. M. Jang, M. H. Jung, J. S. Lee, J. S. Lee, I. C. Lim, H. Im, S. W. Kim, S. A. Kang, W. J. Cho, J. K. Park, *Nanomaterials (Basel)* **2022**, *12*, 2791.
[33] Z. Sun, K. Cheng, F. Wu, H. Liu, X. Ma, X. Su, Y. Liu, L. Xia, Z. Cheng, *Nanoscale* **2016**, *8*, 19644.
[34] D. L. J. Thorek, D. Ulmert, N.-F. M. Diop, M. E. Lupu, M. G. Doran, R. Huang, D. S. Abou, S. M. Larson, J. Grimm, *Nat. Commun.* **2014**, *5*, 3097.
[35] J. C. Park, M. K. Yu, G. I. An, S.-I. Park, J. Oh, H. J. Kim, J.-H. Kim, E. K. Wang, I.-H. Hong, Y. S. Ha, T. H. Choi, K.-S. Jeong, Y. Chang, M. J. Welch, S. Jon, J. Yoo, *Small* **2010**, *6*, 2863.
[36] Y.-D. Xiao, R. Paudel, J. Liu, C. Ma, Z.-S. Zhang, S.-K. Zhou, *Int. J. Mol. Med.* **2016**, *38*, 1319.
[37] C.-H. Huang, A. Tsourkas, *Curr. Top. Med. Chem.* **2013**, *13*, 411.
[38] Z.-R. Lu, *Curr. Opin. Biomed. Eng.* **2017**, *3*, 67.
[39] J. Luo, J. D. Wilson, J. Zhang, J. I. Hirsch, H. C. Dorn, P. P. Fatouros, M. D. Shultz, *Appl. Sci.* **2012**, *2*, 465.
[40] D. Chen, Y. Zhou, D. Yang, M. Guan, M. Zhen, W. Lu, M. E. Van Dort, B. D. Ross, C. Wang, C. Shu, H. Hong, *ACS. Appl. Mater. Interfaces* **2019**, *11*, 21343.
[41] G. Bort, F. Lux, S. Dufort, Y. Crémillieux, C. Verry, O. Tillement, *Theranostics* **2020**, *10*, 1319.
[42] V.-L. Tran, V. Thakare, M. Natuzzi, M. Moreau, A. Oudot, J.-M. Vrigneaud, A. Courteau, C. Louis, S. Roux, F. Boschetti, F. Denat, O. Tillement, F. Lux, *Contrast Media Mol. Imaging* **2018**, *2018*, 7938267.
[43] V. Thakare, V.-L. Tran, M. Natuzzi, E. Thomas, M. Moreau, A. Romieu, B. Collin, A. Courteau, J.-M. Vrigneaud, C. Louis, S. Roux, F. Boschetti, O. Tillement, F. Lux, F. Denat, *RSC Adv.* **2019**, *9*, 24811.
[44] J. Debatisse, O. F. Eker, O. Wateau, T.-H. Cho, M. Wiart, D. Ramonet, N. Costes, I. Mérida, C. Léon, M. Dia, M. Paillard, J. Confais, F. Rossetti, J.-B. Langlois, T. Troalen, T. Iecker, D. Le Bars, S. Lancelot, B. Bouchier, A.-C. Lukasziewicz, A. Oudotte, N. Nighoghossian, M. Ovize, H. Contamin, F. Lux, O. Tillement, E. Canet-Soulas, *Brain. Commun.* **2020**, *2*, fcaa193.
[45] P. Bouziotis, D. Stellas, E. Thomas, C. Truillet, C. Tsoukalas, F. Lux, T. Tsotakos, S. Xanthopoulos, M. Paravatou-Petsotas, A. Gaitanis, L. A. Moulopoulos, V. Koutoulidis, C. D. Anagnostopoulos, O. Tillement, *Nanomedicine (Lond)* **2017**, *12*, 1561.
[46] D. Pan, A. H. Schmieder, S. A. Wickline, G. M. Lanza, *Tetrahedron* **2011**, *67*, 8431.
[47] D. Pan, S. D. Caruthers, A. Senpan, A. H. Schmieder, S. A. Wickline, G. M. Lanza, *Wiley Interdiscip. Rev. Nanomed Nanobiotechnol.* **2011**, *3*, 162.
[48] X. Cai, Q. Zhu, Y. Zeng, Q. Zeng, X. Chen, Y. Zhan, *Int J. Nanomedicine.* **2019**, *14*, 8321.
[49] C. Glaus, R. Rossin, M. J. Welch, G. Bao, *Bioconjug Chem* **2010**, *21*, 715.
[50] J. Zhu, H. Li, Z. Xiong, M. Shen, P. S. Conti, X. Shi, K. Chen, *ACS Appl. Mater. Interfaces.* **2018**, *10*, 34954.
[51] Y. Zhan, S. Shi, E. B. Ehlerding, S. A. Graves, S. Goel, J. W. Engle, J. Liang, J. Tian, W. Cai, *ACS Appl. Mater. Interfaces.* **2017**, *9*, 38304.
[52] Y. Zhan, E. B. Ehlerding, S. Shi, S. A. Graves, S. Goel, J. W. Engle, J. Liang, W. Cai, *J. Biomed. Nanotechnol.* **2018**, *14*, 900.
[53] D. Vecchione, M. Aiello, C. Cavaliere, E. Nicolai, P. A. Netti, E. Torino, *Nanomedicine (Lond)* **2017**, *12*, 2223.
[54] L. W. E. Starmans, M. A. P. M. Hummelink, R. Rossin, E. C. M. Kneepkens, R. Lamerichs, K. Donato, K. Nicolay, H. Grüll, *Adv. Healthcare Mater.* **2015**, *4*, 2137.
[55] L. Xia, X. Guo, T. Liu, X. Xu, J. Jiang, F. Wang, Z. Cheng, H. Zhu, Z. Yang, *Nanoscale* **2019**, *11*, 14400.
[56] L. Xia, X. Meng, L. Wen, N. Zhou, T. Liu, X. Xu, F. Wang, Z. Cheng, Z. Yang, H. Zhu, *Small* **2021**, *17*, e2100378.

[57] Y. Li, T.-Y. Lin, Y. Luo, Q. Liu, W. Xiao, W. Guo, D. Lac, H. Zhang, C. Feng, S. Wachsmann-Hogiu, J. H. Walton, S. R. Cherry, D. J. Rowland, D. Kukis, C. Pan, K. S. Lam, *Nat. Commun.* **2014**, *5*, 4712.
[58] S. Aryal, J. Key, C. Stigliano, M. D. Landis, D. Y. Lee, P. Decuzzi, *Small* **2014**, *10*, 2688.
[59] S. Nagachinta, G. Becker, S. Dammicco, M. E. Serrano, N. Leroi, M. A. Bahri, A. Plenevaux, C. Lemaire, R. Lopez, A. Luxen, M. De La Fuente, *Colloids Surf., B.* **2020**, *188*, 110793.
[60] H. J. Vaughan, C. G. Zamboni, L. F. Hassan, N. P. Radant, D. Jacob, R. C. Mease, I. Minn, S. Y. Tzeng, K. L. Gabrielson, P. Bhardwaj, X. Guo, D. Francisco, M. G. Pomper, J. J. Green, *Sci. Adv.* **2022**, *8*, eabo6406.
[61] M. E. Lobatto, T. Binderup, P. M. Robson, L. F. P. Giesen, C. Calcagno, J. Witjes, F. Fay, S. Baxter, C. H. Wessel, M. Eldib, J. Bini, S. D. Carlin, E. S. G. Stroes, G. Storm, A. Kjaer, J. S. Lewis, T. Reiner, Z. A. Fayad, W. J. M. Mulder, C. Pérez-Medina, *Bioconjug. Chem.* **2020**, *31*, 360.
[62] Z. Körhegyi, D. Rózsa, I. Hajdu, M. Bodnár, I. Kertész, K. Kerekes, S. Kun, J. Kollár, J. Varga, I. Garai, G. Trencsényi, J. Borbély, *Anticancer Res.* **2019**, *39*, 2415.
[63] J.-S. Choi, J. C. Park, H. Nah, S. Woo, J. Oh, K. M. Kim, G. J. Cheon, Y. Chang, J. Yoo, J. Cheon, *Angew. Chem. Int. Ed. Engl.* **2008**, *47*, 6259.
[64] X. Shi, L. Shen, *J. Inorg. Biochem.* **2018**, *186*, 257.
[65] M. Yang, K. Cheng, S. Qi, H. Liu, Y. Jiang, H. Jiang, J. Li, K. Chen, H. Zhang, Z. Cheng, *Biomaterials* **2013**, *34*, 2796.
[66] J. Sun, L. Li, W. Cai, A. Chen, R. Zhang, *ACS Appl. Bio Mater.* **2021**, *4*, 5312.
[67] M. Laprise-Pelletier, M. Bouchoucha, J. Lagueux, P. Chevallier, R. Lecomte, Y. Gossuin, F. Kleitz, M.-A. Fortin, *J. Mater. Chem. B.* **2015**, *3*, 748.
[68] M. S. Kandanapitiye, M. D. Gott, A. Sharits, S. S. Jurisson, P. M. Woodward, S. D. Huang, *Dalton Trans.* **2016**, *45*, 9174.
[69] J. Zhou, M. Yu, Y. Sun, X. Zhang, X. Zhu, Z. Wu, D. Wu, F. Li, *Biomaterials* **2011**, *32*, 1148.
[70] M. I. Tsionou, C. E. Knapp, C. A. Foley, C. R. Munteanu, A. Cakebread, C. Imberti, T. R. Eykyn, J. D. Young, B. M. Paterson, P. J. Blower, M. T. Ma, *RSC Adv.* **2017**, *7*, 49586.
[71] Z. Baranyai, G. Tircsó, F. Rösch, *Eur. J. Inorg. Chem.* **2019**, *2020*, 36.
[72] L. Tian, X. Yi, Z. Dong, J. Xu, C. Liang, Y. Chao, Y. Wang, K. Yang, Z. Liu, *ACS Nano* **2018**, *12*, 11541.
[73] V. Kumar, V. Mundra, Y. Peng, Y. Wang, C. Tan, R. I. Mahato, *Theranostics* **2018**, *8*, 4033.
[74] B. Du, M. Yu, J. Zheng, *Nat. Rev. Mater.* **2018**, *3*, 358.

Huanhuan Liu achieved her Ph.D. degree at the Department of Radiation Science and Technology of Delft University of Technology. She has worked as an assistant researcher in Henan Provincial People's Hospital since 2022. Currently, her research focuses on the design and synthesis of novel PET/MRI probes as well as nanomedicine for combined chemo-radiotherapy. Besides, she is also interested in research focusing on the direct and indirect effects of ionizing radiation.

Meiyun Wang, M.D., Ph.D., is currently working as the vice-president of Henan Provincial People's Hospital. Prof. Wang is the Fellow of the American Institute for Medical and Biological Engineering (AIMBE) and the International Society for Magnetic Resonance in Medicine (ISMRM). She is also the president of the International Society for Neurovascular Disease (ISNVD). She specializes in CT, MRI, PET-CT, and PET-MR diagnosis of various systemic diseases as well as image-guided non-invasive treatment of psychiatric disorders. She is also interested in new medical imaging technologies and the application of AI in medical imaging.